JOURNAL OF SOLID STATE CHEMISTRY **125,** 75–84 (1996)
ARTICLE NO. 0267

Ball Milling-Induced Combustion in Powder Mixtures Containing Titanium, Zirconium, or Hafnium

L. Takacs

Department of Physics, University of Maryland Baltimore County, Baltimore, Maryland 21228-5398

Received February 22, 1996; in revised form May 13, 1996; accepted May 14, 1996

Ball milling induces self propagating high temperature reactions in many highly exothermic powder mixtures. This phenomenon has been studied in a variety of reactions with titanium, zirconium, and hafnium. Several oxides (CuO, Cu_2O, NiO, Fe_3O_4, and ZnO) were reduced with Ti, Zr, and Hf and the borides, carbides, silicides, and sulfides of these metals were prepared from elemental mixtures. The ignition time is much shorter with Zr than with either Ti or Hf whenever oxygen or sulfur is involved in the reaction, but no similar variation is observed for the formation of borides, carbides, and silicides. It is suggested that the fast diffusion of oxygen in ZrO_2 and very likely of sulfur in ZrS_2 are responsible for this behavior.

INTRODUCTION

Combustion has been initiated by ball milling in a variety of highly exothermic reaction mixtures. The formation of metal chalcogenides (1, 2), NiAl (3), $MoSi_2$ (4, 5), Ti carbides (6), and TiB_2 (7) from their elemental components accelerates during ball milling to become a self-sustained high temperature reaction. Mechanochemical reactions between a reactive metal and the oxide (8–12) or chloride (13) of another metal can also become combustive.

During the first phase of the process, milling results in attrition, mixing, and mechanochemical activation of the reactants. At some point ignition occurs and the reaction continues as a self propagating high temperature synthesis (SHS) (14). Understanding the ignition process and estimating the activation time before ignition is of considerable interest. Combustion and the resulting high temperatures have to be avoided in most mechanochemical syntheses, for example if metastable or energetic materials are prepared. Mechanical activation can also be combined with an SHS reaction. In that case, the process is easier to control if the activation and combustion steps are physically separated (15).

The ignition of combustion during ball milling is a very complicated phenomenon. Two general conditions have to be met: (1) the mechanical action of an individual impact must be capable of initiating a chemical reaction and (2) the heat generated by the mechanical action and the chemical reaction locally must be sufficient to start a combustion wave, which can propagate into adjoining material outside the impact zone. The first condition can be investigated in terms of the principles of mechanochemistry (16); the second part of the process is described by the theory of SHS reactions (14). Whether these conditions are met depends on many elementary processes. They include structure refinement by mixing, deformation, attrition, and cold welding (17, 18); the formation of lattice defects (19); chemical reactions at the interfaces (20); and heat conduction (21). The dynamics of the mill (22, 23), and the mechanical (24) and thermochemical (9) properties of the reactants must be considered.

The exothermicity of a reaction is usually described in terms of the adiabatic temperature. It is defined as the temperature increase due to the reaction heat, if the reaction takes place in an isolated system. A combustion wave can propagate if the heat generated by the reaction increases the temperature above a critical value, sufficient to initiate further reaction in a neighboring unreacted volume element. If heat conduction is neglected, the condition of combustion can be stated as a requirement that the adiabatic temperature exceeds a critical value (9). As expected, the adiabatic temperature also correlates with the activation time before the ignition of combustion. If the other properties of the reactants and the milling conditions are similar, ignition usually occurs more easily, i.e., after a shorter milling time, in the more exothermic reaction mixture. However, this correlation fails in many cases, indicating that other properties must also play an important role (12). An interesting example is the combination reaction of Zn and S as a function of composition. While the adiabatic temperature is obviously the highest at the composition of the only product phase, ZnS, the shortest activation time was measured at the molar ratio of Zn/S = 2 (25).

Although the adiabatic temperature is not the only parameter controlling the initiation of combustion, it is usually the dominant one. Therefore, in order to study the

0022-4596/96 $18.00

role of any other material property, reactions with similar thermodynamic parameters must be compared. Simple combination and displacement reactions with the metals of the IVB column of the periodic table, Ti, Zr, and Hf, are especially promising: These metals participate in reactions with identical stoichiometries, the reaction heats are very similar. Many of their reactions are exothermic enough to support combustion. For example, if the oxide of a less reactive metal is reduced with one of the IVB metals, the driving force of the reaction equals the difference between the enthalpies of formation of the two oxides. The enthalpies of formation for TiO_2, ZrO_2, and HfO_2, are -472, -550.5, and -559 kJ/mole of oxygen atom, similar to each other and much larger than the corresponding values for, e.g., Fe_3O_4 and CuO, -277 and -162 kJ/mole of oxygen atom (26). The similarities go well beyond reaction heats. Each metal of the IVB column has the same hcp crystal structure at room temperature and transforms to bcc at elevated temperature. Their mechanical and chemical properties—especially those of Zr and Hf—are very similar. The equilibrium phase diagrams are also similar for Ti, Zr, and Hf containing systems (27).

Preliminary investigations have shown that the mechanochemical reduction of Fe_3O_4 and Cu_2O is combustive with all three IVB metals, and the activation times are an order of magnitude shorter with Zr than with either Ti or Hf (28). It was suspected that this surprising difference originated from the fast oxygen diffusion in ZrO_2. Contrasting behavior was observed by Park *et al.* during the mechanochemical synthesis of diborides from elemental mixtures (7). Combustion was observed during the preparation of TiB_2, but ZrB_2 formed with gradual kinetics.

In order to elucidate the reasons for this behavior, a set of mechanochemical reactions was investigated. Several oxides—CuO, Cu_2O, NiO, Fe_3O_4, and ZnO—were reduced with Ti, Zr, and Hf. The large variation of the enthalpy of formation from CuO to ZnO results in a wide range of driving forces of the reactions. The mechanochemical preparation of borides, carbides, silicides, and sulfides was also investigated. An initial account of this work was presented earlier (29).

The reaction heat normalized to one mole of nonmetal, ΔH, and $\Delta H/C$, a simplified ''adiabatic temperature,'' are listed in Table 1 for the investigated reactions. Here C is the room temperature heat capacity of the products. The thermodynamic parameters were taken from Ref. (26); data were not available for the formation of HfS_2, ZrSi, and HfSi. (The room temperature heat capacity of TiC is unreasonably large in Ref. (26). This is probably a misprint; the value given by Ref. (30) is used instead. The agreement between the two sources is good for the other two carbides.) The quantity $\Delta H/C$ is calculated instead of the true adiabatic temperature. This is acceptable, as this parameter is used only to characterize self heating close to room temperature. Of course, neglecting the latent heats results in unrealistically high ''temperatures'' with no direct physical significance. The true adiabatic temperature has to be calculated if not only ignition but also the propagation and products of the reaction are studied. An advantage of using $\Delta H/C$ is the availability of dependable data; the very high temperature properties needed to evaluate adiabatic temperatures are often not known or they may be inaccurate.

EXPERIMENTAL

The milling experiments were performed using SPEX 8000 Mixer/Mills (SPEX Industries, Inc.) and round bottom hardened steel vials. The starting powders and steel balls were placed into the vial in an argon-flushed glove box to avoid excessive oxidation. The following materials were used: Ti (99.9%, -100 mesh), Zr (99%, -325 mesh), Hf (99.5% except for 2–3% Zr, -325 mesh), CuO (99%, -200 mesh), Cu_2O (97%, -325 mesh), NiO (99%, -325 mesh), Fe_3O_4 (97%), ZnO (99.8%, -325 mesh), B (99.99%, -325 mesh), C (99.5%, -300 mesh), Si (99.5%, -325 mesh), and S (precipitated, -60 mesh). All materials were obtained from Johnson Matthey. For combination reactions, the molar ratio of the reactants corresponded to the reaction stoichiometry. In order to compensate for oxygen contamination, the quantity of the reducing metal was increased by 10% for the displacement reactions.

The progress of the reactions was monitored by measuring the temperature with a type K thermocouple attached to the outside surface of the vial. The ignition of combustion is indicated by a sudden increase in the temperature. In some experiments, several thermocouples were attached to different parts of the milling vial. The temperature jump was recorded within one second by all thermocouples. Combustion generates audible sound, which is also noticed at the same moment when the sudden temperature increase is recorded. The time from starting the mill to the sudden temperature increase—the ignition time—is the primary quantity discussed in this paper. The reproducibility of the ignition times is usually better than 10%, except for the fastest reactions.

The number and size of the milling balls was chosen to obtain convenient milling times (between about 5 min and 1 h in most cases.) Much shorter activation times are difficult to measure accurately. The large (L), medium (M), and small (S) ball sizes refer to 12.7 mm, 9.52 mm, and 6.4 mm diameters, the most typical choices were 3 L, 5 M, or 5 L balls. The mass of the powder charge was 3 g in most experiments. In the case of the metal–boron mixtures, a series of experiments with constant nominal reactant volume was also performed.

The phase composition of the reaction products was investigated by X-ray diffraction using a Philips X-ray generator, Cu$K\alpha$ radiation, and a vertical goniometer. Either

TABLE 1
Reaction Heat per Nonmetal, ΔH, and the Simplified "Adiabatic Temperature," $\Delta H/C$, for the Investigated Reactions

Reaction	M = Ti		M = Zr		M = Hf	
	ΔH (kJ/mol)	$\Delta H/C$ (K)	ΔH (kJ/mol)	$\Delta H/C$ (K)	ΔH (kJ/mol)	$\Delta H/C$ (K)
$2CuO + M \rightarrow 2Cu + MO_2$	−310	6000	−389	7400	−397	7300
$2NiO + M \rightarrow 2Ni + MO_2$	−232	4300	−311	5700	−319	5700
$Fe_3O_4 + M \rightarrow 3Fe + 2MO_2$	−195	4200	−273	5800	−282	5800
$2Cu_2O + M \rightarrow 4Cu + MO_2$	−299	3900	−377	4900	−386	4900
$2ZnO + M \rightarrow 2Zn + MO_2$	−122	2300	−200	3700	−208	3700
$M + 2S \rightarrow MS_2$	−204	6000	−289	8400		
$M + 2B \rightarrow MB_2$	−158	7100	−162	6700	−164	6600
$M + C \rightarrow MC$	−185	5400	−207	5500	−226	6000
$M + Si \rightarrow MSi$	−129	2900				

Note. C is the room temperature heat capacity of the products. Most data are taken from Ref. (26). The heat capacity of TiC is from Ref. (30).

a NaI scintillation detector or an intrinsic Ge detector was used. The contributions of the $K\alpha_1$ and $K\alpha_2$ radiations were not separated.

In order to correlate the ignition times with the thermal behavior of the reactions, several heating curve measurements were performed. The powders were mixed thoroughly by milling for 3 min with 10 small balls. The mechanochemical activation resulting from this treatment is negligible. Some of the powder mix was placed into a small length of thin-walled stainless steel tube under argon and the ends of the tube were sealed by folding them back and pressing with a hydraulic press. The sample obtained this way was heated in a tube furnace while its temperature was recorded with a thermocouple.

RESULTS

The vial temperature measured during the mechanochemical reduction of Fe_3O_4 with Zr is shown in Fig. 1 as a function of milling time. Similar curves have been obtained during all reactions. The instant of ignition is clearly indicated by the abrupt temperature increase; the time from the start of milling to this moment is defined as the ignition time, T_{ig}. The two curves represent temperatures measured at two different points on the milling vial. The abrupt temperature increase occurs within the same one-second sampling interval at both points. The shapes of the two curves are quite different, indicating large temperature differences during and immediately after combustion.

The ignition times are given in Table 2 for the mechanochemical reactions investigated in this work. The size of the powder charge and the number and size of the milling balls are also given. Ignition times obtained under different conditions cannot be compared directly. The reactions can be classified into two groups: (1) Oxidation–reduction reactions and sulfidation ignite after a short activation time if the metal component is Zr; the ignition times are much longer with Ti or Hf. The difference is a factor of three or larger, except for the reduction of ZnO. (2) The ignition time varies monotonically from Ti to Zr to Hf for the formation of diborides and carbides. When preparing silicides, the ignition time is the shortest with Zr, but the ignition time with Hf is longer by less than 20%.

Collecting data on a large number of systems is important to facilitate the separation of main trends from

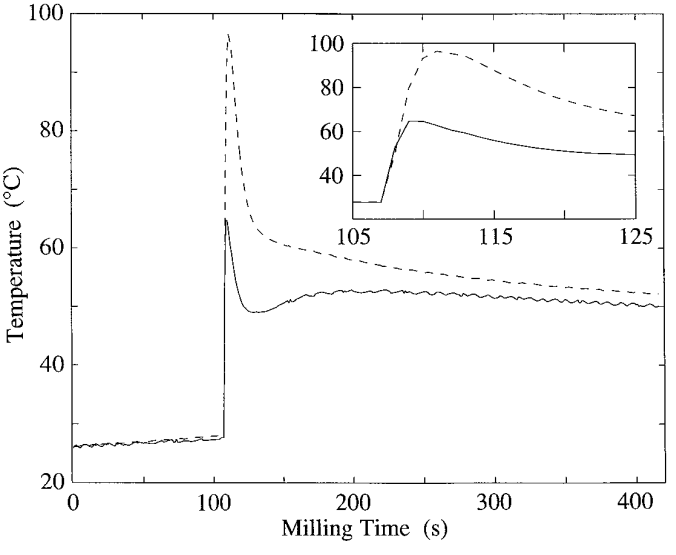

FIG. 1. The temperature measured at the top and at the bottom of the milling vial during the mechanochemical reduction of Fe_3O_4 with Zr. The insert shows the point of ignition on a finer time scale.

TABLE 2
Activation Time before the Ignition of Combustion, T_{ig}, for Several Reactions with Ti, Zr, and Hf.

Reaction	Milling conditions		T_{ig} (sec)		
	Powder	Balls	M = Ti	M = Zr	M = Hf
$2CuO + M \rightarrow 2Cu + MO_2$	3 g	3 L	60	15	50
$2NiO + M \rightarrow 2Ni + MO_2$	3 g	3 L	570	90	470
$Fe_3O_4 + M \rightarrow 3Fe + 2MO_2$	3 g	3 L	570	50	130
$2Cu_2O + M \rightarrow 4Cu + MO_2$	3 g	3 L	1730	60	1980
$2ZnO + M \rightarrow 2Zn + MO_2$	3 g	3 L	5860	3160	4500
$M + 2S \rightarrow MS_2$	3 g	5 M	8820	17	250
$M + 2B \rightarrow MB_2$	3 g	5 M	3600	2760	1850
$M + C \rightarrow MC$	3 g	5 L	3120	2570	2180
$M + Si \rightarrow MSi$	3 g	5 L	1620	840	1030
$2Cu_2O + M \rightarrow 4Cu + MO_2$	3 g	10 S	5860	400	4800
$Fe_3O_4 + M \rightarrow 3Fe + 2MO_2$	6 g	6 L	1190	110	320
$M + 2B \rightarrow MB_2$	0.334 cc	5 M	1260	1840	1850

Note. Large (L), medium (M), and small (B) balls refer to 12.7 mm, 9.52 mm, and 6.4 mm diameters.

secondary details and experimental artifacts. In this way, data from several rows or columns of Table 2 can be compared to test the validity of relationships.

X-ray powder diffraction phase analysis has been performed on all reaction products. The samples represent a rather ill-defined state after the high temperature reaction and some additional milling. Yet, they reflect the differences between the investigated systems. The products may also give clues concerning the route of the reactions. In some cases, milling was interrupted shortly before the moment when ignition was expected to occur, and the phase composition of the sample was investigated in this ''critical'' pre-combustion state. Some typical results are shown in Figs. 2–5.

The X-ray powder diffraction patterns obtained after the combustive mechanochemical reduction of Fe_3O_4 with Ti, Zr, and Hf are shown on Fig. 2. The samples contain a small amount of unreacted metal and Fe_3O_4; the main products are Ti_3O_5, ZrO_2, or HfO_2, relatively little α-Fe is found. The product with Ti contains an unidentified orthorombic phase (a = 3.716 Å, b = 4.271 Å, c = 6.277 Å), probably a mixed oxide. The products with Zr and Hf also contain an unidentified phase, but only two lines are well-resolved (at 30.4° and 43.2°) and this information is not sufficient to identify the structure.

The results on the other oxide systems are qualitatively similar. The following general observations can be made: (1) The reactions are not complete; some unreacted metal, mixed oxide, and/or Fe_3O_4 are present. Higher reaction temperatures result in more complete reactions. The temperature is higher during the more exothermic reactions (e.g., with CuO) and during the faster reactions with Zr, which allow less time for heat loss to the milling tools. (2) Monoclinic ZrO_2 or HfO_2 are the main oxide products when the reducing metal is Zr or Hf. Titanium can form a variety of oxides; rutile (tetragonal TiO_2) or monoclinic Ti_3O_5 dominate depending on the other component. (3) Many diffraction lines could not be identified. Probably most of them originate from mixed oxides. As these samples are always mixtures of several phases, they are not suitable for the identification of new phases.

The simplest diffractograms have been obtained after the combustive mechanochemical reactions with carbon (Fig. 3.) NaCl type carbides are the only product phase, except for some unreacted Hf. This is not particularly surprising. These carbides are stable within a wide composition range below 50% (27); they can probably also accommodate impurities without the formation of new phases. The lattice parameters are slightly smaller than those given by the JCPDS cards. The difference, 0.17, 0.19, and 0.30% for TiC, ZrC, and HfC, suggests carbon deficiency (30). The broadening of the diffraction lines reflects small particle size (and probably lattice strain) induced by the continued milling after combustion. Differences in the length and intensity of milling resulted in different linewidths for the three carbide samples. The broadest lines were observed in the case of HfC. The integral breadth method revealed that small particle size is the dominating source of line broadening; the estimated average diameter is about 200 nm.

The diboride samples are dominated by the expected product phase, but they also contain unidentified impurity phases. The reason is that the diborides are essentially line

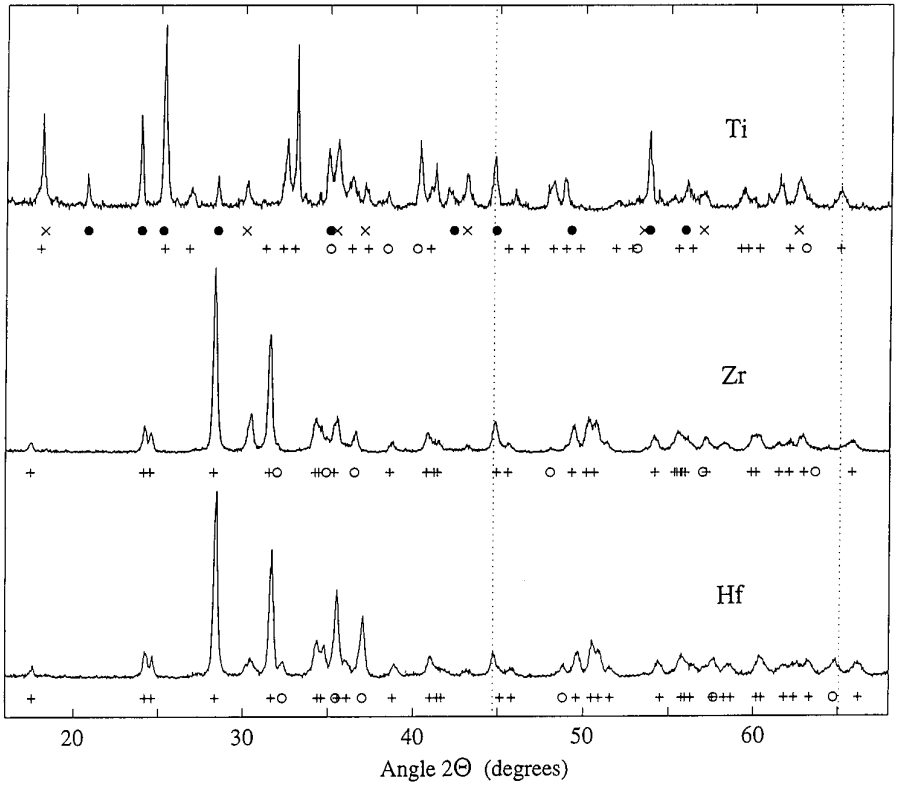

FIG. 2. X-ray powder diffractograms after the combustive reduction of Fe_3O_4 with Ti, Zr, and Hf. Unreacted Ti, Zr, and Hf (○); Ti_3O_5, ZrO_2, and HfO_2 (+); and some α-Fe (vertical dotted lines) were identified in each sample. The product with Ti also contains some unreacted Fe_3O_4 (×) and an unidentified orthorombic phase (●). Some lines of the products with Zr and Hf (e.g., the ones at 30.4° and 43.2°) could not be identified.

compounds (27), which cannot accommodate impurities or off-stoichiometry. The diffraction pattern of ZrB_2 is shown on Fig. 4 as an example. The upper curve was measured on a Zr–B mixture milled for about 90% of the expected ignition time. It is dominated by the broadened lines of Zr except for a minor shoulder at 32.4°. Obviously, very little if any chemical change took place during the mechanical activation period.

The powder diffractograms of the Ti–S and Zr–S reaction products are shown on Fig. 5; the result for the Hf–S system is almost indistinguishable from the Zr–S pattern. Both samples are dominated by unreacted metal and sulfur. Not a single resolved titanium sulfide line could be found, and the presence of zirconium sulfide (probably Zr_3S_2) is indicated only by two moderately intense lines near 30° and 40°. This surprising result indicates that combustion was limited to a small fraction of the sample volume and very little reaction product was formed. The temperature increase measured on the surface of the vial was also very small, smaller than for most combustion reactions. As the formation of sulfides is the most exothermic group of reactions in this study, the small temperature increase is quite unexpected but it is consistent with the incomplete reactions found by X-ray diffraction. The reason for this behavior may be the low boiling temperature of sulfur. When the reaction begins, the temperature at the Zr–S interface increases and the sulfur evaporates, thereby separating the reactants. It is remarkable that the ignition time is much shorter with Zr than with either Ti or Hf, similarly to the oxidation–reduction reactions, in spite of this unusual behavior (Table 2).

The thermal initiation of explosive solid state reactions was studied in mixtures of Fe_3O_4 and CuO with Ti, Zr, and Hf. Typical heating curves are shown on Figs. 6 and 7. The reproducibility of the ignition temperatures was only about 50°C due primarily to variations in the packing of the powder. In spite of this uncertainty, the much lower ignition temperature of the Zr containing mixtures is apparent with both oxides. Ignition did not occur in CuO–Hf mixtures up to 1020°C. Measurements were also attempted on metal–sulfur and metal–boron mixtures. Unfortunately, sulfur boiled off the sample before combustion and the ignition temperature of boride formation exceeded the maximum temperature of the furnace used in these experiments.

DISCUSSION

The first phase of mechanochemical reactions involves attrition, mixing, and mechanochemical activation. As X-

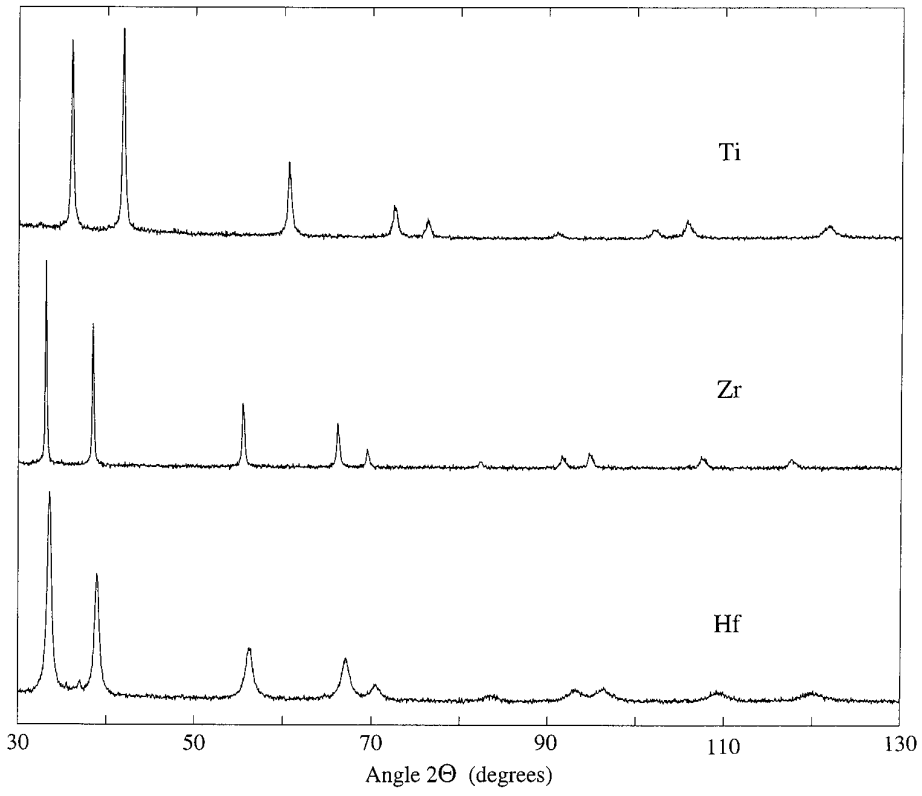

FIG. 3. X-ray powder diffractograms of the product after combustive mechanochemical reaction of Ti, Zr, and Hf with carbon. All the main diffraction lines originate from cubic TiC, ZrC, and HfC. A very small amount of unreacted Hf is present.

ray diffraction measurements performed on samples taken shortly before ignition indicate, very little chemical change occurs during this phase (see Fig. 4a and Refs. (2, 10)). At some point the reaction rate starts to increase. It may continue as a faster, but still gradual reaction, or ignition may occur. Combustion may extend to a single particle only and remain undetected, or it may propagate through the volume of the powder. The investigation of the changes leading to ignition contributes to understanding the processes during the activation time in combustive and noncombustive reactions alike.

Correlation between Ignition Time and Thermodynamic Parameters

Among the parameters influencing the activation time before ignition, the thermochemical properties of the reaction are the most significant. The reaction heat is the driving force of the process; $\Delta H/C$—the simplified ''adiabatic temperature''—describes self heating, which is a key element of the propagation of combustion. In fact, a minimum adiabatic temperature is often used as a simple necessary condition of combustion in SHS processes (9). Therefore, correlations between the thermodynamic parameters (Table 1) and the ignition time (Table 2) are discussed before considering any other property.

The largest consistent set of ignition time data has been collected on displacement reactions with oxides using 3 g of powder and 3 L balls. The results are plotted as a function of $\Delta H/C$ in Fig. 8. The most obvious trend is the expected decrease of the ignition time for the more exothermic reactions. The lower adiabatic temperatures may also partly explain why the ignition times are longer for the reactions with Ti than with Zr. This explanation has to be taken with caution, though, because there is little overlap between the data for Ti and Zr. If the data points representing the reduction of CuO with Ti (the most exothermic reaction with Ti) and the reduction of ZnO with Zr (the least exothermic reaction with Zr) are removed, a wide gap remains between the results for Ti and Zr. The ignition times of the reactions involving Hf are significantly longer, and the difference cannot be explained by thermodynamic differences. (This difference is not an artifact caused by oxidation or an impurity in the hafnium starting powder. Such a problem would also influence the ignition times of boride and carbide formation, where a similar variation is not observed.)

Thermodynamic parameters can also explain some trends of the combination reactions. The formation of car-

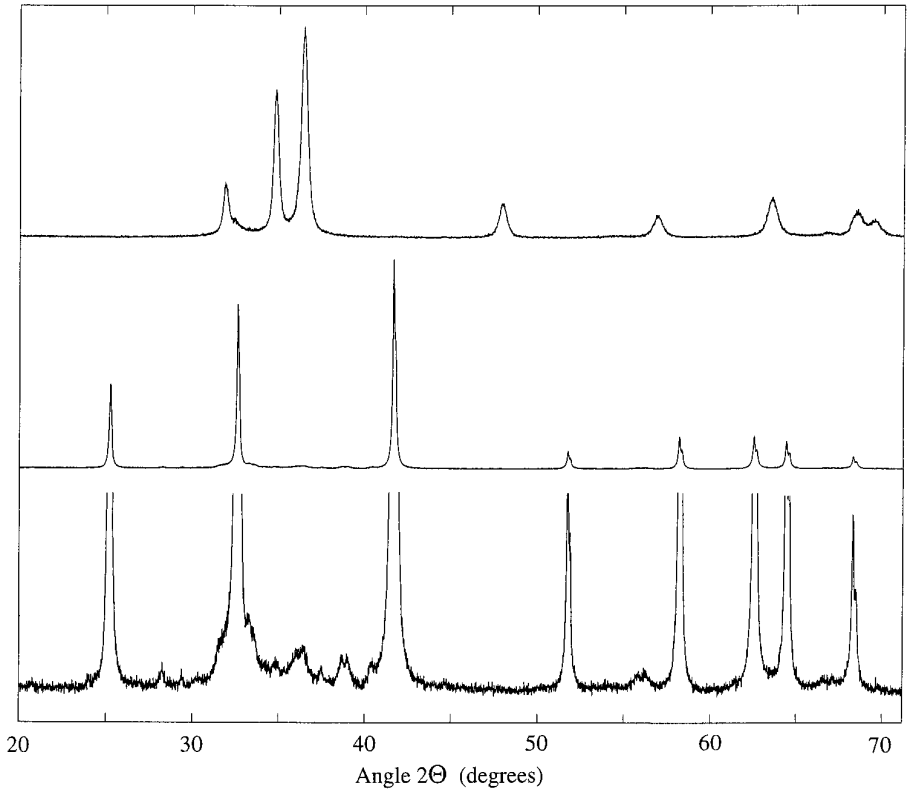

FIG. 4. X-ray powder diffractograms immediately before (upper curve) and after (middle curve) the combustive reaction between zirconium and boron. All lines of the upper curve, except the shoulder at 32.4°, originate from unreacted zirconium. The main lines of the middle curve originate from hexagonal ZrB_2. The lower curve presents the same diffraction pattern on a more sensitive scale to show the weak lines of the impurity phase(s).

bides is less exothermic than the formation of diborides. As a consequence, higher milling intensity—larger milling balls—were needed to achieve comparable ignition times. The reactions involving Ti are usually somewhat less exothermic than the reactions with either Zr or Hf. The only exception is the formation of TiB_2, which is more exothermic than the formation of ZrB_2 or HfB_2. This fact can explain why combustion could be induced with Ti but not with Zr during Park's attempt to prepare diborides via lower energy ball milling (7). The ignition time observed in our constant volume series of diboride preparation is also much shorter with Ti than with Zr or Hf. The low value of $\Delta H/C$ fails to explain the relatively short ignition times for silicide formation.

The Role of Diffusion

The very short ignition times for the reactions of Zr with oxides and with sulfur but not with B, C, and Si cannot be explained by differences of the thermochemical parameters. The explanation has to include a process which (a) distinguishes Zr from Ti and Hf and (b) relates to its interaction with other elements, promoting fast reactions with oxides and sulfur but not with boron and carbon. Such a process is the diffusion of the nonmetal in the product phase. CaO stabilized ZrO_2 is used as a solid electrolyte, based on the fast diffusion of oxygen ions (31). The diffusion coefficient of oxygen is also anomalously large in ZrO_2 (32) and very likely sulfur diffuses easily in ZrS_2. On the other hand, the diffusion coefficients of B in borides and C in carbides are not drastically different for Ti and Zr compounds (32, 33). This difference correlates well with the observed trend of the ignition times.

Available data on diffusion coefficients were collected and related to the systematics of ignition times earlier (29). Instead of using experimental diffusion coefficients, the structure of the appropriate compounds will be compared in this discussion. More open structures usually allow for faster diffusion. An advantage of this approach is the availability of accurate data. It also circumvents the problem of using bulk diffusion data for a case where the presence of lattice defects influences diffusion significantly.

The atomic diameters usually increase down the columns of the periodic table, but column IVB is a notable exception. Zr is larger than Ti as expected, but Hf, being immediately after the lanthanides, is smaller than Zr, in spite of the much larger number of its electrons. The atomic

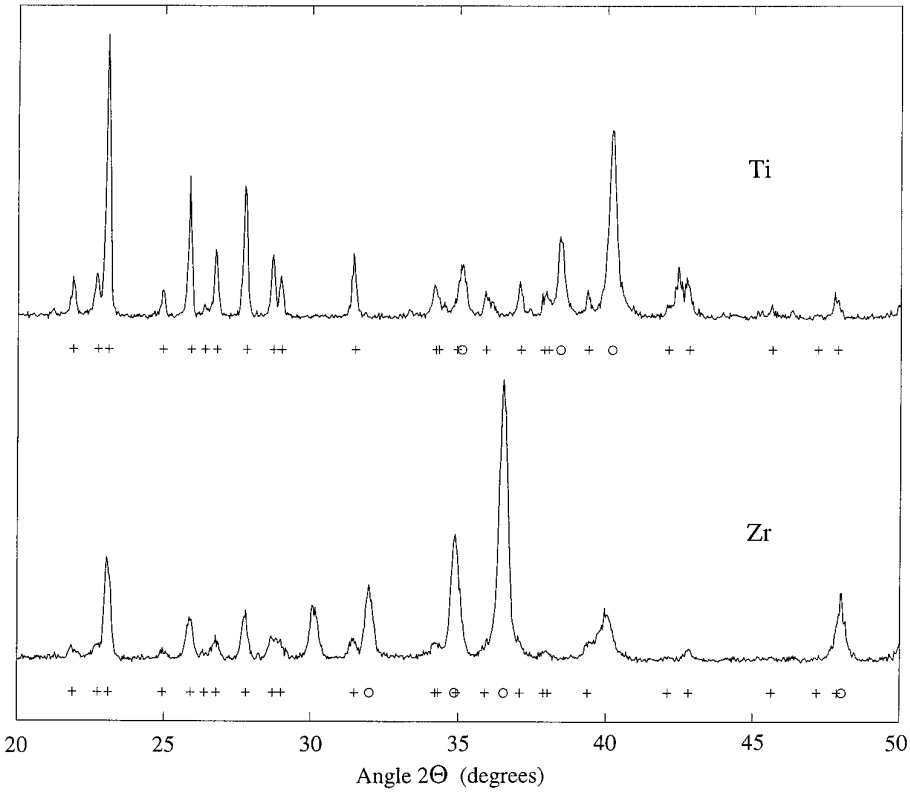

FIG. 5. X-ray powder diffraction after the combustive reaction of sulfur with Ti and Zr. The line positions of Ti or Zr (○) and S (+) are indicated.

volumes in hexagonal Ti, Zr, and Hf are 17.7, 23.3, and 22.1 Å^3, respectively. The volume per formula unit varies similarly for any set of Ti, Zr, and Hf compounds, being the largest for the Zr compound. However, this variation conceals a more subtle trend. Subtracting the volume of the metal atom from the volume of a compound molecule, the effective volume per nonmetal atom can be calculated. Lattice structure data were taken from Ref. (34); the results for MO_2, MS_2, MSi, MB_2, and MC (M = Ti, Zr, or Hf) are shown in Fig. 9. The atomic volumes of oxygen and sulfur are the largest in the Zr compounds, indicating that the structure of these compounds is more open than the structure of Ti and Hf oxides and sulfides, allowing for faster diffusion. This difference is in addition to the size difference of the metal atoms. No similar trend exists for the borides, carbides, and silicides. (The ignition time is slightly shorter for the Zr–Si mixture than for the Ti–Si and Hf–Si mixtures. An analysis of reaction heats and phase relationships may rationalize the difference; diffusion is probably not the explanation.)

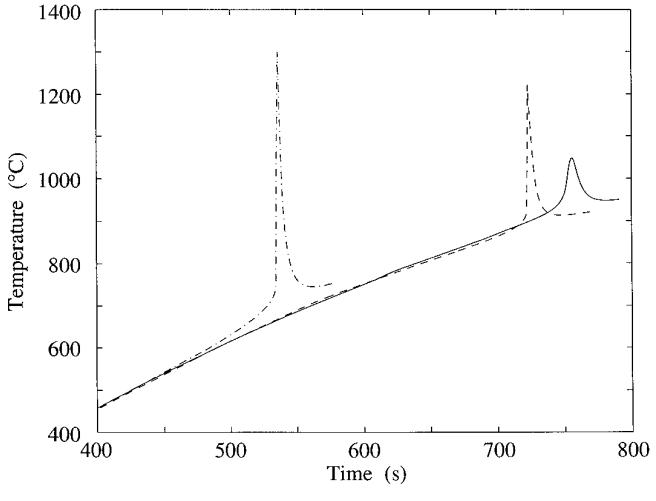

FIG. 6. Heating curves for powder mixtures of Fe_3O_4 with Ti (full line), Zr (dot-dashed line), and Hf (dashed line).

The different diffusion rates in Ti, Zr, and Hf oxides should influence the kinetics of ordinary solid state reactions, not only the ones induced by mechanical activation. Much shorter ignition times were indeed found when Fe_3O_4 and CuO were reduced with Zr, rather than Ti or Hf (Figs. 6 and 7.) The thermal ignition of explosive reactions was analyzed by Atzmon (35). He showed that not only diffusion through the product layers but also through interfacial diffusion barriers needs to be considered when describing self-sustained reactions.

Diffusion influences the ignition of combustion in several

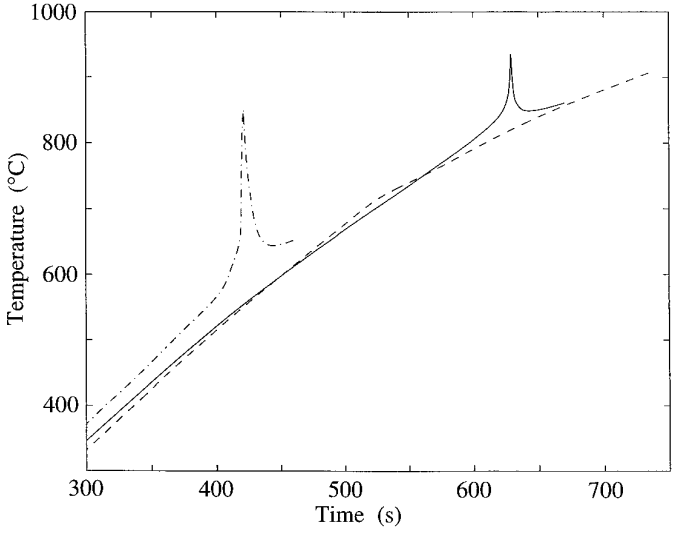

FIG. 7. Heating curves for powder mixtures of CuO with Ti (full line), Zr (dot-dashed line), and Hf (dashed line).

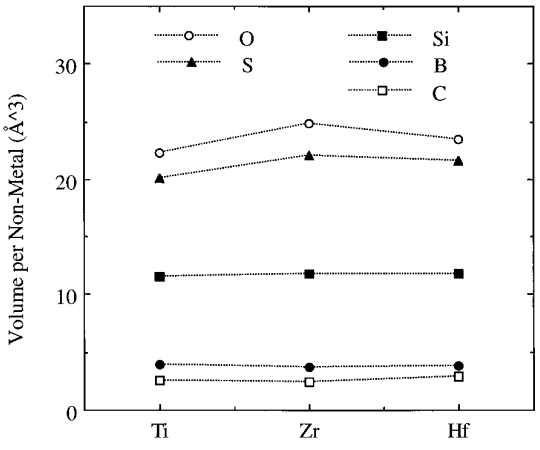

FIG. 9. Atomic volume per nonmetal for the dioxides, diborides, carbides, monosilicides, and disulfides of Ti, Zr, and Hf.

ways. General thermodynamic considerations show that interdiffusion at the interface is a prerequisite of the nucleation and growth of any new phase (36). Diffusion occurs at the impact site both during and following the collision of the milling balls. Matter transport is also one of the key processes during the propagation of the combustion wave (14).

The ignition of combustion also depends on the mechanical properties of the reactants (37). Overly ductile materials tend to form large particles and cover the surface of the balls and the milling container, thereby decreasing the efficiency of milling. On a microscopic level, higher ductility promotes the formation of interfaces between the component particles. On the other hand, the collision between hard particles may result in more highly excited reaction sites. The mechanical properties of Ti, Zr, and Hf are similar; the variation across the rows of Table 2 may not originate from differences in hardness or ductility.

Some peculiarities of the ignition time data of Table 2 remained unexplained. The ignition times for the reduction of NiO and Fe_3O_4 are equal with Ti, but there is a large difference if Hf is the reducing metal. The difference between Zr and the other two IVB metals is extremely large for the reduction of Cu_2O but small for the reduction of ZnO. The reactions with Si are relatively fast compared to the formation of carbides. The explanation of these features requires further investigations.

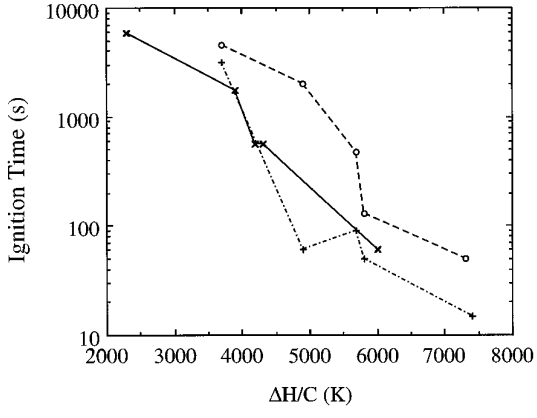

FIG. 8. Ignition time as a function of $\Delta H/C$ for the reduction of oxides with Ti (× and full line), Zr (+ and dot-dashed line), and Hf (○ and dashed line).

X-Ray Diffraction Phase Analysis

Although the results of the X-ray diffraction phase analysis show a variety of interesting behaviors, these are largely unrelated to the variation of the ignition time. The displacement reactions with oxides are often incomplete, and intermediate mixed oxides are formed in many systems. The monocarbides have a broad stability range; the diborides are practically line compounds; the IVB metal–silicon phase diagrams include a large number of compound phases with a variety of compositions and crystal structures. As a consequence, the carbide products are single phase, the boride products are dominated by the diborides but contain impurity phases, and the reactions with silicon produce complicated mixtures of several phases, none of them dominant. These differences in phase composition do not seem to influence the variation of the ignition time.

The case of sulfide formation is particularly interesting. Combustion does occur, but it extends only to a small fraction of the sample volume, probably due to the easy evaporation of sulfur. As shown recently (38), the remaining unreacted powder makes a series of combustion

reactions possible in the same powder as milling is continued. Each, except the last one, extends to only a fraction of the sample volume. However, the processes preceding the first ignition occur in the solid state. Consequently, the shortest ignition time is measured with Zr, regardless of the fact that combustion is quenched after having extended to a small fraction of the sample volume only. Interestingly, other sulfur and sulfide systems are among the most widely studied mechanochemical reactions (1, 2, 39–42).

CONCLUSIONS

The ignition of combustion depends on several variables, e.g., the exothermicity of the reaction as characterized by the adiabatic temperature (9); parameters defining the milling intensity, i.e., the type of mill, the number and size of the milling balls, and the ball to powder ratio (12); and the refinement of the microstructure (18). As demonstrated in this study, diffusion at the interface between the reactant particles is also important. The combustive mechanochemical reactions of Ti, Zr, and Hf can be divided into two well defined categories: Reactions requiring the diffusion of oxygen or sulfur are very fast if the metal component is Zr, but slower if it is Ti or Hf. The ignition time of the reactions with boron, carbon, or silicon only slightly depends on the metal component. We suggest that this behavior is related to the more ''open'' structure of Zr oxide and sulfide and the ensuing faster diffusion.

Many reactions (9×3) have been investigated in this work. This made the identification of trends possible, in spite of experimental uncertainties and the many parameters influencing the reactions. The results will also serve as a guide when selecting systems for more detailed studies.

ACKNOWLEDGMENTS

This work was supported by DRIF funds provided by the University of Maryland Baltimore County. The technical assistance of Mark A. Susol and Mohan Singh is appreciated.

REFERENCES

1. Chr. G. Tschakarov, G. G. Gospodinov, and Z. Bontschev, *J. Solid State Chem.* **41,** 244 (1982).
2. L. Takacs and M. A. Susol, *J. Solid State Chem.* **121,** 394 (1996).
3. M. Atzmon, *Phys. Rev. Lett.* **64,** 487 (1990).
4. E. Ma, J. Pagán, G. Cranford, and M. Atzmon, *J. Mater. Res.* **8,** 1836 (1993).
5. S. N. Patankar, S-Q. Xiao, J. J. Lewandowski, and A. H. Heuer, *J. Mater. Res.* **8,** 1311 (1993).
6. A. A. Popovich, V. P. Reva, V. N. Vasilenko, V. A. Maslyuk, and T. A. Popovich, *Inorg. Mater.* **29,** 434 (1993).
7. Y. H. Park, H. Hashimoto, T. Abe, and R. Watanabe, *Mater. Sci. Eng. A* **181/182,** 1291 (1994).
8. G. B. Schaffer and P. G. McCormick, *J. Mater. Sci. Lett.* **9,** 1014 (1990).
9. G. B. Schaffer and P. G. McCormick, *Mater. Sci. Forum* **88–90,** 779 (1992).
10. L. Takacs, *Mater. Lett.* **13,** 119 (1992).
11. T. D. Shen, K. Y. Wang, J. T. Wang, and M. X. Quan, *Mater. Sci. Eng. A* **151,** 189 (1992).
12. L. Takacs, *in* ''Nanophase and Nanocomposite Materials'' (S. Komarnemi, J. C. Parker, and G. J. Thomas, Eds.), MRS Symp. Proc. Vol. 286, p. 413, 1993.
13. H. Yang and P. G. McCormick, *J. Mater. Sci. Lett.* **12,** 1088 (1993).
14. A. G. Marzhanov, *in* ''Combustion and Plasma Synthesis of High-Temperature Materials'' (Z. A. Munir and J. B. Holt, Eds.), p. 1. VCH Publishers, New York, 1990.
15. G. T. Hida and I. J. Lin, *in* ''Combustion and Plasma Synthesis of High-Temperature Materials'' (Z. A. Munir and J. B. Holt, Eds.), p. 246. VCH Publishers, New York, 1990.
16. G. Heinicke, ''Tribochemistry.'' Hauser, München, 1984.
17. B. J. M. Aikin and T. H. Courtney, *Metall. Trans. A* **24,** 2465 (1993).
18. R. Maric, K. N. Ishihara, and P. H. Shingu, *Mater. Sci. Forum* **179–181,** 801 (1995).
19. V. V. Boldyrev, *Solid State Ionics* **63–65,** 537 (1993).
20. V. Boldyrev and E. Boldyreva, *Mater. Sci. Forum* **88–90,** 711 (1992).
21. D. R. Maurice and T. H. Courtney, *Metall. Trans. A* **21,** 289 (1990).
22. R. W. Rydin, D. Maurice, and T. H. Courtney, *Metall. Trans. A* **24,** 175 (1993).
23. M. Magini, *Mater. Sci. Forum* **88–90,** 121 (1992).
24. C. C. Koch, *Annu. Rev. Mater. Sci.* **19,** 121 (1989).
25. L. Takacs and M. A. Susol, *Mater. Sci. Forum*, in press.
26. O. Kubaschewski, C. B. Alcock, and P. J. Spencer, ''Materials Thermochemistry,'' 6th ed. Pergamon Press, Oxford, 1993.
27. T. B. Massalski, (Ed.), ''Binary Alloy Phase Diagrams,'' American Society of Metals, Metals Park, Ohio, 1986.
28. L. Takacs, ''123rd TMS Annual Meeting and Exhibition,'' p. 26. San Francisco, 1994.
29. L. Takacs, *Mater. Sci. Forum*, in press.
30. E. K. Storms, ''The Refractory Carbides.'' Academic Press, New York, 1967.
31. Per Kofstad, ''Nonstoichiometry, Diffusion, and Electrical Conductivity in Binary Metal Oxides,'' p. 137. Wiley–Interscience, New York, 1972.
32. O. Kubaschewski, *in* ''Zirconium: Physico-Chemical Properties of its Compounds and Alloys'' (K. L. Komarek, Ed.), Atomic Energy Rev., Special Issue No. 9, p. 263. International Atomic Energy Agency, Vienna, 1976.
33. O. Kubaschewski, *in* ''Titanium: Physico-Chemical Properties of its Compounds and Alloys'' (K. L. Komarek, Ed.), Atomic Energy Rev., Special Issue No. 6, p. 441. International Atomic Energy Agency, Vienna, 1983.
34. W. B. Pearson, ''Handbook of Crystallographic Data for Intermetallic Phases.'' American Society of Metals, Metals Park, OH, 1985.
35. M. Atzmon, *Metall. Trans. A* **23,** 49 (1992).
36. J. Philibert, *Defect Diffusion Forum* **95–98,** 493 (1993).
37. E. G. Avvakumov and N. V. Kosova, *Siberian J. Chem.* **5,** 62 (1991).
38. L. Takacs, *Appl. Phys. Lett.*, in press.
39. E. G. Avvakumov, ''Mechanical Methods of the Activation of Chemical Processes,'' p. 154. (Nauka, Novosibirsk, 1986.
40. P. Baláz, T. Havlik, Z. Bastl, and J. Briancin, *J. Mater. Sci. Lett.* **14,** 344 (1995).
41. T. Kosmac and T. H. Courtney, *J. Mater. Res.* **7,** 1519 (1992).
42. S. H. Han, K. A. Gschneidner, Jr., and B. J. Beaudry, *Scripta Metal. Mater.* **24,** 295 (1990).